Cardiovasc Intervent Radiol (1981) 4:117–123

CardioVascular and Interventional Radiology

A Fully Automated Determination of the Left Ventricular Region of Interest in Nuclear Angiocardiography

Michael L. Goris, James H. McKillop, and Philippe A. Briandet
Stanford University School of Medicine Stanford, California, USA

Abstract. The precise delineation of the left ventricular projection area is an essential part in the quantitative analysis of nuclear angiocardiograms. We have devised an algorithm that permits automation of this step, based on a one-dimensional Laplace operator whose kernel is 2, 2, −2, −4, −2, 2, 2. The operator characteristically enhances "valleys" more than edges and, therefore, favors septal and the valve plane detection. The operator is applied vertically, horizontally, and along both diagonals. Each pass is immediately followed by a local maximum search during which the image resulting from the Laplacian operator is reduced to a binary one, with zeros everywhere except where a local maximum was found along the path of the operator.

This resultant image yields a closed "edge" around the left ventricle, even though many structures outside the left ventricle are also delineated. However, the centroid of the ventricle is defined from functional criteria and the region of interest is defined from centroid to first edge.

The method has been applied to first-pass and gated studies in anterior and 45° left anterior oblique views. In 100 successive cases the ejection fraction obtained automatically was compared to the manual result. The regression equation yielded the relation: automatic method (%) = 1.7 + 1.0 manual method (%) ± 2% ($r = 0.995$), which is not significantly different from the identity relation. The failure rate was low (13%) but varied from 28% in first-pass studies in the anterior view, to less than 8% in gated studies in the left anterior oblique projection.

Key words: Heart, ventricles – Heart, radionuclide studies – Nuclear medicine

During scintigraphic analysis of left ventricular (LV) function in nuclear angiocardiography, changes in left ventricular volumes are derived from changes in count rates. This derivation is based on the realization that for an equilibrated intravascular tracer, the concentration remains constant in the left ventricular cavity during the complete contraction cycle and that the same is true for a first-pass study during systole, inasmuch as the tracer is uniformly mixed within the ventricular cavity. Under those circumstances and if self-absorption remains constant, changes in left ventricular activity can be due only to changes in left ventricular volume.

Further analysis, however, requires that left ventricular count rates be sampled without bias and with exclusivity. The requirement of exclusivity cannot truly be met because of overlap or "crosstalk," and is usually approximated by background correction or thresholding [1]. Sampling without bias requires that the total ventricular projection area be included in the sampling area but, to facilitate exclusivity, that other major structures be avoided. The definition of the left ventricular sampling area or region of interest (ROI) has been shown to be crucial [2] and is in general performed in an interactive way by a skilled user.

In this paper we present a method which is fully automated and user[1] independent. The main advantage is universality: the effect of local processing particularities is eliminated. Furthermore, automation al-

James H. McKillop is a Harkness Fellow of the Commonwealth Fund of New York

Address reprint requests to: Michael L. Goris, M.D., Ph.D., Division of Nuclear Medicine, Stanford University School of Medicine, Stanford, CA 94305, USA

1 The term "user" is used for human operator while the term "operator" is reserved for mathematical functions

0174-1551/81/0004/0117/$01.40

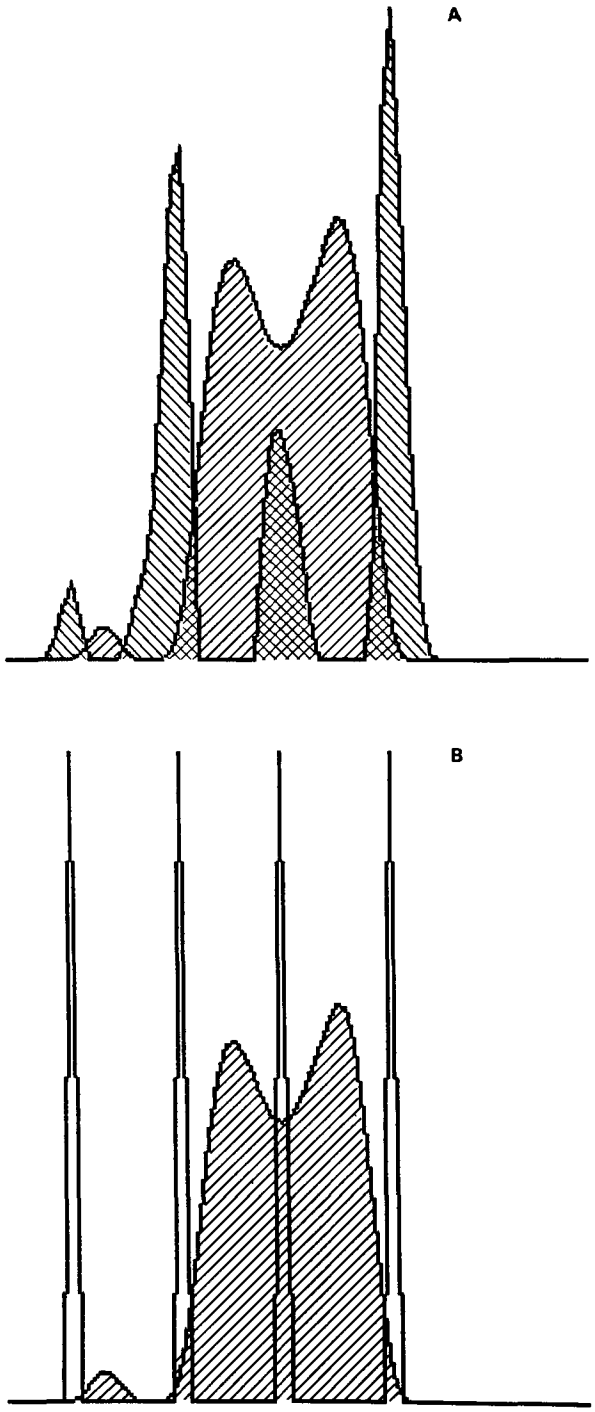

Fig. 1A, B. Illustration of convolution and local maximum search. **A** A horizontal count profile through an end-diastolic reference image is shown superimposed on the corresponding profile in the convolution image. One notes a small non-cardiac structure as well as the right and left ventricles in the reference image. The convolution image has four structures, the major ones at the free ventricular borders and one corresponding to the septum. **B** In this image the binary edges are superimposed on the count profile of the reference image. All detected edges are of equal magnitude. To detect the left ventricular region, it is sufficient to start a search anywhere between the septum and the free wall's edge. The start of the search is based on functional criteria.

lows batch processing, and the processing time is not influenced by user availability. The advantages of automation, however, exist only to the extent that automation matches a skilled user for accuracy.

The method is based on a search for a closed edge surrounding the ventricular projection area. The distinction between ventricular edges and edges from other structures is made exclusively on topographic criteria: for a search starting within the left ventricular projection area, the first closed edge is the ventricular edge.

The definition of edges is performed by using a pseudo-Laplacian convolution operator. This unidimensional operator is applied four times and each time immediately followed by local maximum search which reduces all edges to the same amplitude.

Materials and Methods

Scintigraphic data accumulated during first-pass or equilibrium (electrocardiographic) gated nuclear angiocardiography using a standard size scintillation camera (Ohio Nuclear) were reconstructed as a set of 16 frames (64 × 64 pixel). Each frame contained the cumulative data from one of 16 equivalent time segments in six (first-pass) or more (gated) cardiac cycles [2, 3].

Thus the set of 16 frames constituted the temporal and spatial representation of the count rate distribution at different times of the cardiac cycles, and is further referred to as the cycle image.[2]

Prior to the search for the left ventricular region of interest, this cycle image was smoothed in object space using a nine point operator (−3, 2, 6, 8, 9, 8, 6, 2, −3) applied successivley in the two spatial and in the temporal directions. Following this, all frames of the cycle image were thresholded according to a non-interactive algorithm described elsewhere. The algorithm, which was based on a search for a threshold between moving and stationary structures in the cycle image, substracted a single constant value from each picture element (pixel) of each frame of the cycle image [4].

The search for the left ventricular borders ultimately used to define the LV region of interest was performed twice. The first time the search was performed on a reference image, which was the frame in the cycle image corresponding to the time of end diastole. The second time the reference image was obtained by addition of the values in corresponding pixels of the 16 frames of the cycle image. The second reference image was, therefore, the image of the spatial count rate distribution, averaged over the total cardiac cycle.

In each case the reference image was a matrix A (64, 64). The convolution operator (O) was applied to the reference image A sequentially in the horizontal, vertical, and two diagonal directions. The kernel of O was (2, 2, −2, −4, −2, 2, 2). To reduce the effect of noise in the reference image, the operator was applied to the average of three pixels in A, orthogonally to the operator's pathway.

Thus, in the resultant image B of the horizontal pass, the element $B(K, L)$ was defined by

$$B(K,L)=\sum_{J=L-1}^{J=L+1}\sum_{I=1}^{I=7} O(I)\cdot A(K-4+I,J).$$

2 The term "image" is used strictly; the cycle image is the mapping of the temporal and spatial count rate distribution during the cardiac cycle

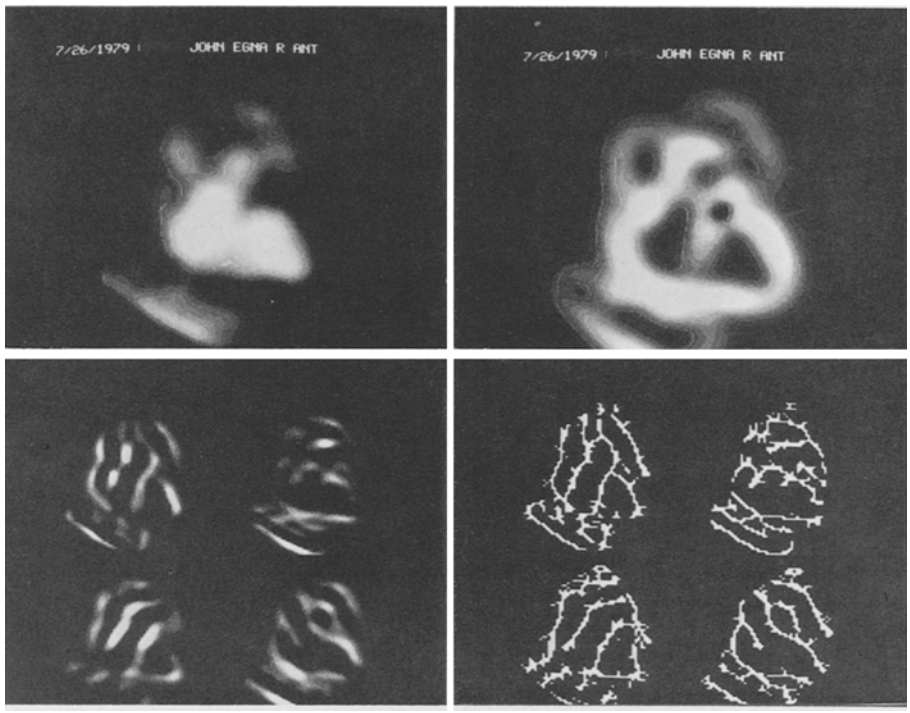

Fig. 2. Illustration of edge-finding algorithm. This figure illustrates the progression of the algorithm applied to the end-diastolic reference image of an anterior equilibrium gated study (*top left*). The results of the convolution for each direction are shown in the left lower quadrant. One notes that the "edges" have varying intensities. To each convolution image a local maximum search is applied in the corresponding direction. The resulting images (*right lower quadrant*) now contain sharp (binary) edges of constant intensity. In the upper right quadrant the sum of the four original convolutions is shown. This image (not used by the algorithm) is analogous to gradient images and contains ambiguities at the junction of more than two edges. Furthermore, if one tried to track the ventricular border by following the largest crest, one would miss the septum.

For the diagonal pass (upper left to lower right), the image elements of the resultant image were defined as

$$B(K, L)=\sum_{J=1}^{J=3}\sum_{I=1}^{I=7} O(I)\cdot A(K+I+J-6, L+I-J-2).$$

The same logic was used, with appropriate changes, for the vertical and the other diagnonal pass (Fig. 1).

Following each operator pass, negative values were set to zero and a search for local maxima was started along the pathway of the operator. The local maxima were defined over three points; hence, in the horizontal direction the location (K, L) was a local maximum if any of the following conditions was satisfied:

$$B(K-1, L)\leqq B(K, L)>B(K+1, L)$$

$$B(K-1, L)<B(K, L)\geqq B(K+1, L).$$

If the coordinate (K, L) contained a local maximum in any pass, the element $G(K, L)$ of a binary image, originally set to zero, was given the value 1 (Figs. 1 and 2).

After four passes the image G was such that the ventricular projection area contained only zero values, or isolated non-zero values, but was surrounded by a closed border of non-zero values (Figs. 3 and 5). Because other vascular structures, as well as the left ventricle were also surrounded by a closed border, the identification of the LV further required an approximate starting point for the border search within the LV projection area. This initial search position was found by computing the X and Y coordinates of the center of gravity of a functional image representing the contraction amplitude. This image was constructed as follows: Pixel values in the end-systolic frame were subtracted from values in corresponding pixels of the end-diastolic frame. In the resultant image, negative values were suppressed. This resulted in an image in which pixels in the projection area of the ventricles contained positive values, since the count rate density decreased from diastole to systole in the ventricular regions, while it tended to remain constant or increase in all other regions. In the gated studies the initial position was corrected by a search for the first local maximum to the right in the end-diastolic frame, since the center of gravity could be over the right ventricle or the septum.

From each reference image (end diastole or cycle summation), a separate region of interest was defined in this manner. The septum was better detected in the cycle summation image; the atrium was better separated in the end-diastolic image. The final left ventricular region of interest was the intersection of the two defined regions of interest.

Acquisition and data processing were performed by a dedicated nuclear medicine computer. The system had a 32K, 16-bit word memory and was hard disc based (SIMIS-4).

The method was evaluated by comparing the automatically drawn region to that drawn manually by a "skilled" user. This user is the physician in our laboratory who processes most of the studies. In a first step, the regions were visually compared. If there were gross discrepancies, a failure was scored. Gross discrepancies were defined as the inclusion of the right ventricle, left atrium, or aortic root or the obvious exclusion of part of the left ventricle. The remaining cases were scored as successes, even if the manual and automatic methods were slightly dissimilar. In the successful cases, the ejection fractions obtained by both methods were compared by regression analysis.

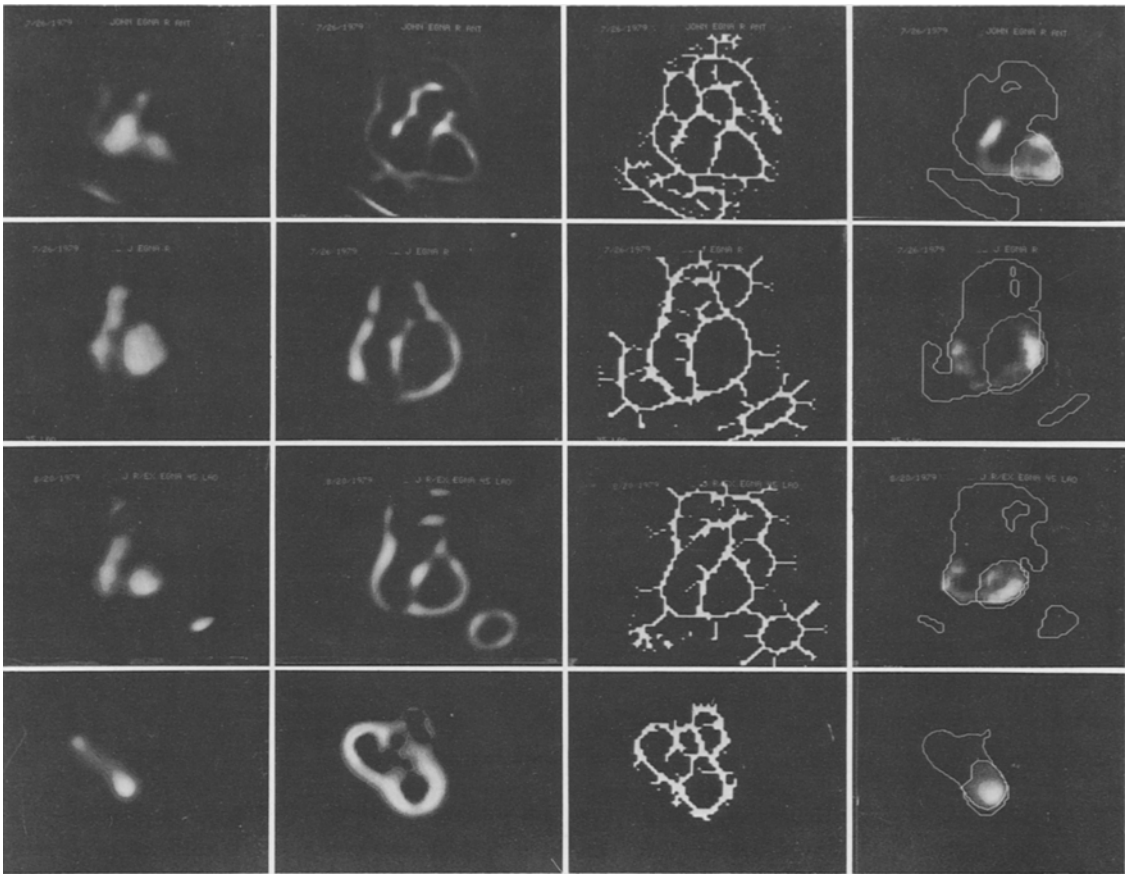

Fig. 3. Illustration of region of interest definition. This figure illustrates the results of the four-pass convolution and summated local maximum search (image G in the text) on four cases (gated study: anterior, LAO, LAO; first-pass study: LAO). The last column shows the functional image (regional stroke volume) superimposed on the tracings of the blood pool above threshold and of the final region of interest. This figure illustrates how the selection of the final LV region of interest depends on a search whose initial position is defined by the functional image.

Results

The success rate of the method is tabulated in Table 1. For those cases only, the regression analysis between the manual and automatic methods yielded a slope of 1.0 and an intercept of 1.7(%). The standard error of the estimate was 2%. The relation was not significantly different ($P>0.2$) from an identity relation. The correlation coefficient was 0.99. The overall suc-

Table 1. Success rate of left ventricular region of interest determination

	Projections		
	ANT	LAO	Total
FPNA	72% (8/11)	86% (19/22)	81% (27/33)
EGNA	76% (13/17)	92% (58/63)	88% (71/80)
Total	75% (21/28)	91% (77/85)	86% (98/113)

FPNA: First pass study: EGNA: Gated blood pool study; ANT: Anterior; LAO: 45° left anterior oblique

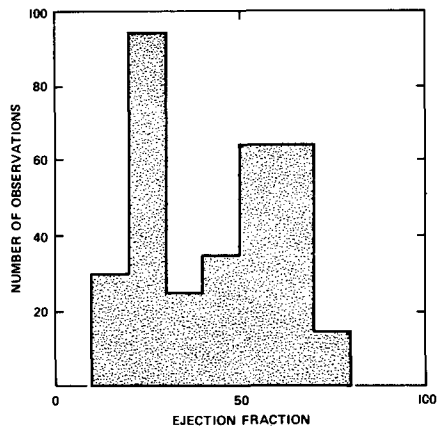

Fig. 4. Frequency distribution of ejection fractions in the cases tested. The distribution of failures did not significantly differ from that of successes, demonstrating that the method is independent of LV function. Specifically, if one compares ejection fraction intervals 0–30%, 31–50%, and 51–100%, the failures over success are 6/32, 4/21, 8/42, yielding a chi-square value of 0.001 ($P>0.3$, for 2 degrees of freedom)

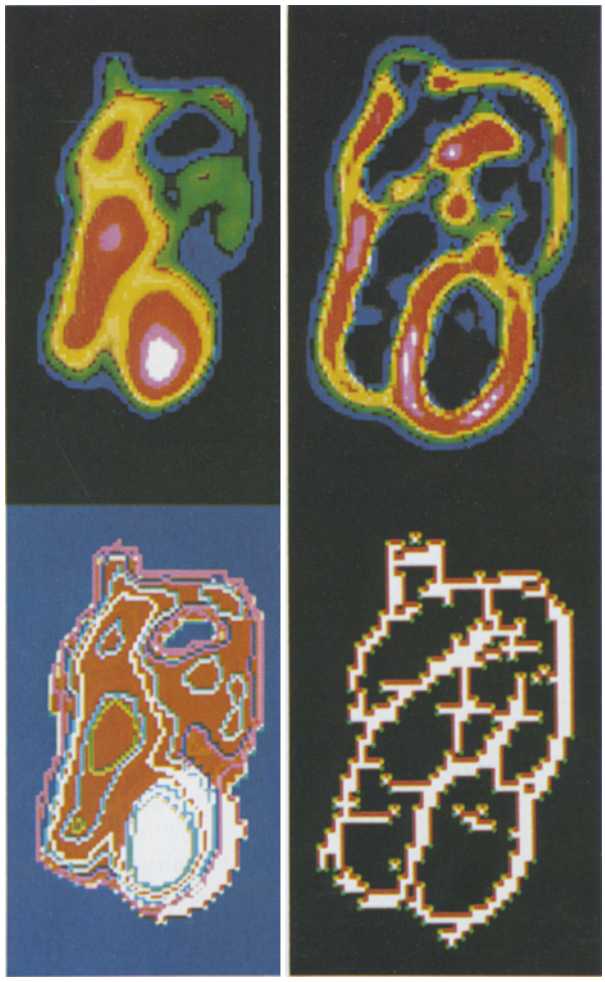

Fig. 5. In the upper left quadrant the cycle summation image is shown. A large left ventricle is easily distinguished from all other sturctures. This is underscored by the summation of the four Laplacian images in the upper right quadrant: the septal edge has an amplitude equal to that of the free wall. In the lower right quadrant the binary image G is shown. The closed area, corresponding to the LV, is shown in white in the left lower quadrant. Superimposed we see different isocount lines. The isocount lines that identify the septum do not properly identify the free wall.

cess rate was 86%, with the lowest success achieved with the first-pass technique in the anterior projection (72%) and the highest with the gated technique in the 45° left anterior oblique projection (92%).

The success rate was independent of the left ventricular function. In Figure 4 the frequency distribution of the ejection fraction in the tested cases is shown. Ejection fractions ranged from 15% to 80%. This distribution was not different in the successful cases as tested by a chi-square test (chi-square = 0.001, degrees of freedom = 2, $P > 0.3$). Figure 5 demonstrates how the final left ventricular region of interest cannot be selected by thresholding. In this case, with a very obvious septum and a convolution image that would allow one to track the edge through the septum (as opposed to the case in Fig. 2), one cannot define all ventricular borders by a single isocount line (lower left quadrant).

Discussion

Criteria for the determination of left ventricular sampling regions are mainly morphological [5–7], but functional criteria have been described [4, 8, 9]. The functional criteria are easily included in an automated approach but may fail if a large part of the LV is nonfunctional (akinetic or dyskinetic). Additionally, in gated studies, the right ventricle's kinetics are not qualitatively different from those of the left ventricle since the right ventricle contracts in phase with the left ventricle.

The left ventricle's projection area is circumscribed by a local decrease in count rate, either as a dip (septum, valve plane) or an edge; a number of methods for defining the left ventricle have been based on this fact. Cahill [10] has described an edge detector based on nearest neighbors that is user independent in the kidneys. An application in cardiac studies has not been described since in both first-pass and gated studies the left ventricular border is not necessarily the only edge or the one with the greatest amplitude. This problem is underscored by work by O'Connor based on the "bordon" [11] and by Jones based on slope and isocount levels [12]. In each case a priori boundaries have to be set by the operator, and the problem is artificially reduced to finding the border within a predefined LV region. Bounding has been done automatically on the basis of functional criteria by Douglas [13, 14]. In this case bounding is performed on the basis of row and column signature in the functional image, showing end-diastolic minus end-systolic counts. The method requires, therefore, a fairly normal wall motion distribution.

The physical assumptions underlying the present approach are simple: The ventricle is assumed to be a recognizable structure superimposed on a monotone background (tissue crosstalk) and surrounded by other structures from which it is separated by valleys. In each case there is an abrupt change in the first derivative perpendicular to the ventricular border. The physical assumptions are not competely satisfied since there still exists partial overlap between important cardiac structures, for example, the septum and left atrium. Sometimes there remains an apparent border, which is selected. Most failures are due to the lack of such a border, in which case operator-

Table 2. Illustration of the convolution operator

Picture element number	Kernel element	Count		Convolution	
		Case 1	Case 2	Case 1	Case 2
1	2	4	1	8	2
2	2	3	2	6	4
3	−2	2	3	−4	− 6
4	−4	1	4	−4	−16
5	−2	2	3	−4	− 6
6	2	3	2	6	4
7	2	4	1	8	2
SUM				+16	−16

Table 2 illustrates the convolution of the pseudo-Laplacian operator's kernel in two cases. In case 1, the image profile is concave, in case 2 convex. The convolution value (SUM) is found by adding the result of the multiplication of corresponding kernel and image elements, e.g., for case 1: $16=(2\times4)+(2\times3)-(2\times2)-(4\times1)-(2\times2)+(2\times3)+(2\times4)$. The convolution value is placed in element No. 4 in the resultant image. In true Laplacians, the operator is two-dimensional. Thus, in the case of a saddle point, i.e., when case 1 and 2 are perpendicular to each other and superimposed in element No. 4, the Laplacian would be zero.

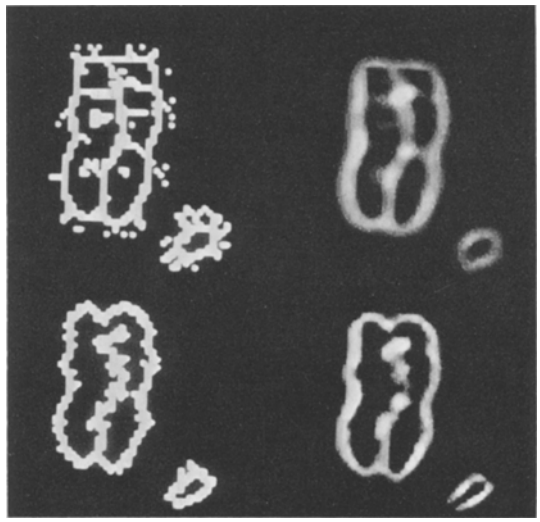

Fig. 6. This figure illustrates the difference between two-dimensional operators (gradient search) and sequential one-dimensional operators in the detection of edges. On the left the binary edges are shown, derived from the one-dimensional pseudo-Laplacian operator (*top*) and from a two-dimensional operator. Close examination reveals s that small edges orthogonal to large edges tend to remain undetected in the two-dimensional operator

defined regions of interest suffer from a certain degree of arbitratiness and the automatic method fails.

For this one-dimensional operator, the data are count profiles, taken in the X, Y, or either diagonal direction. The operator is symmetrical so that an edge detected from within the ventricle (in-to-out) would be identical to one directed from out of the ventricle (out-to-in). The operator detects concavity versus convexity. The profile through (monotone) tissue crosstalk is neither concave nor convex. The profile perpendicular to the septum is concave at the septum. Within the ventricle profiles are, in general, convex. At the border of the ventricle the profile perpendicular to the border is concave. The results of the convolution are illustrated in Table 2 for two cases.

The separate convolution along four profiles is an important feature of our approach. The case of the septum illustrates the point: The septum is concave in the count profile to which it is perpendicular only. True (two-dimensional) Laplacians or gradient images tend to average the effects of the profile's characteristics in two directions (Fig. 6). This is not the case here. Since each convolution is followed by a local maxima search, the profiles are analyzed truly independently. Finally, the particular enhancement of valleys by this convolution should be noted. The detection of the free wall whose shape tends to be 0, 0, 0, 1, 2, 3, 3 is easy by almost any method. The septal valley, even if it has a smaller amplitude (i.e., 2, 2, 2, 1, 2, 2, 2) is equally enhanced by this filter which yields +4 for the former and for the latter (see Table 2). The present method also overcomes the problem of edge size and uniqueness by the local maxima search and the definition of LV from its centroid to the first closed border.

The relative independence of the method from left ventricular function is demonstrated by the wide range of ejection fractions in successful cases (Fig. 4). Failure is usually due to the lack of a perceptible separation between ventricle and outflow tract or atrium. User intervention in these cases is totally based on preconceived anatomical criteria rather than on actual observations, except in those cases in which the functional image can be trusted [4, 8, 9]. In a few cases of hyperkinetic ventricles, the region of interest derived from the cycle summation image appears too small (counted as failure).

In general, failure is obvious (e.g., inclusion of aorta) and not frequent enough to deter from first attempt, considering that the processing of one gated study requires 165 seconds.

References

1. Goris ML (1979) Non-target activities: Can we correct for them? Teaching Editiorial. J Nucl Med 20:1312–1314
2. Marshall RC, Berger HJ, Costin JC, Freedman GS, Wolberg HJ, Cohen LS, Gottschalk A, Zart BL (1977) Assessment of cardiac performance with quantitative radionuclide angiocardiography. Circulation 56:820–829
3. Maddox DE, Wynne J, Uren R, Parker JA, Idoine J, Siegel LC, Neill JM, Cohn PF, Holman BL (1979) Regional ejection fraction: A quantitative radionuclide index of regional left ventricular performance. Circulation 59:1001–1009
4. Goris ML (1978) Non-interactive identification of the left ven-

tricular area. Presented at Symposium on Selected Computer Aspects of Nuclear Cardiology. Mid-winter Meeting, Society of Nuclear Medicine, Atlanta, GA, January 19–23
5. Schelbert HR, Verba JW, Johnson AD, Brock GW, Alazraki NP, Rose FJ, Ashburn WL (1975) Nontraumatic determination of left ventricular ejection fraction by radionuclide angiocardiography. Circulation 51:902–909
6. Strauss HW, Pitt B (1977) Gated cardiac blood-pool scan: use in patients with coronary artery disease. Prog Cardiovasc Dis 20:207–216
7. Ashburn WL, Schelbert HR, Verba JW (1978) Left ventricular ejection fraction – a review of several radionuclide angiographic approaches using the scintillation camera. Prog Cardiovasc Dis 20:267–284
8. Green MV, Brody WR, Douglas MA, Borer JS, Ostrow HG, Line BR, Bacharach SL, Johnston GS (1978) Ejection fraction by count rate from gated images. J Nucl Med 19:880–883
9. Geffers H, Adam WE, Bitter F, Sigel H, Kampmann H (1978) Data processing and functional imaging in radionuclide ventriculography. Proceedings of First International Conference on Information Processing in Medical Imaging, June 1977, Nashville, Tennessee. National Technical Information Service, U.S. Department of Commerce, Springfield, Virginia, pp 322–332
10. Cahill P, Ho L, Ornstein E, Becker DV (1977) Operator independent edge detection algorithms in nuclear medicine. Proceedings of the 24th Annual Meeting, Society of Nuclear Medicine, Chicago, June 1977. J Nucl Med 18:607
11. O'Connor JL, Kronenberg MW, Higgins SB, Pederson RW, Rhea TC (1979) A new method for count-based border definition which emulates visual function-application to radionuclide ventriculography. Proceedings of the 26th Annual Meeting, Society of Nuclear Medicine, Atlanta, GA, June 1979. J Nucl Med 20:642
12. Jones JP, Price RR, Rollo FD (1979) A simple edge-finding algorthm for gated cardiac images. Proceedings of the 26th Annual Meeting, Society of Nuclear Medicine, Atlanta, GA, June 1979. J Nucl Med 20:643
13. Douglas MA, Green MV (1978) A system for computer generation of left ventricular masks for use in computerized ECG-gated radionuclide angiocardiography. Proceedings Symposium on Nuclear Cardiology: Selected Computer Aspects, Atlanta, GA, 1978. Society of Nuclear Medicine, New York, pp 119–128
14. Douglas MA, Green RV, Ostrow HG (1978) Evaluation of automatically generated left ventricular regions of interest in computerized ECG-gated radionuclide angiocardiography. Computers in Cardiology, Stanford, California, 1978, IEEE Publishing Services, New York, pp 201–204